

# Determination of Association Rate Constants by an Optical Biosensor Using Initial Rate Analysis

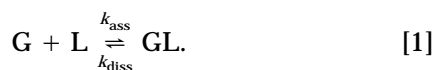
Paul R. Edwards\* and Robin J. Leatherbarrow†<sup>1</sup>

\*Affinity Sensors, Saxon Way, Bar Hill, Cambridge, CB3 8SL, United Kingdom; and †Biological Chemistry, Department of Chemistry, Imperial College of Science, Technology and Medicine, South Kensington, London, SW7 2AY, United Kingdom

Received April 23, 1996

**We show that initial rate analysis can be successfully applied to analyze experimental binding data generated by an optical biosensor. The initial rates of binding obtained from linear regression are concentration dependent, and plots of initial rate against ligate concentration yield a straight line that passes through the origin. The slope of this graph is the product of the association constant times the maximal binding capacity of the immobilized ligand. This latter parameter is easily obtained from a single binding curve at high ligate concentration, allowing rapid determination of the association rate constant. The association rate constant obtained in this manner is found to be in good agreement with that obtained by the more customary method of nonlinear regression analysis of the entire binding profile. Initial rate analysis is more simple than fitting the full association profile and needs less data collection time. It also requires fewer assumptions about the functional form of the association profile. This can be advantageous when fitting biosensor-derived data, which often show complex association kinetics. Furthermore, it avoids the potential complication of second-order kinetics which may be found at low ligate concentrations with high-affinity interactions.** © 1997 Academic Press

The determination of kinetic parameters for protein–protein interactions as described by Eq. [1] is an important aspect in the characterization of a biological system.



In this scheme,  $k_{\text{ass}}$  is the association rate constant and  $k_{\text{diss}}$  is the dissociation rate constant. The dissocia-

tion equilibrium constant,  $K_D$ , is the ratio of these terms (Eq. [2]).

$$K_D = \frac{k_{\text{diss}}}{k_{\text{ass}}} \quad [2]$$

There are several experimental techniques that allow the calculation of  $K_D$  for a reaction equilibrium. However, the measurement of uncomplexed interactant (G or L) often requires the labeling of one of the interactants together with a separation stage to remove unbound, labeled protein. Optical biosensors (1, 2) not only allow the  $K_D$  value to be determined but also provide the individual rate constants ( $k_{\text{ass}}$  and  $k_{\text{diss}}$ ) of the reaction. In general, these instruments require one component, the ligand, to be covalently linked to the sensing surface, typically via attachment to an intermediate hydrogel layer. The other protein in solution, the ligate, then binds to this immobilized ligand. These methods offer several advantages over the more conventional techniques for measuring kinetic constants, such as enzyme-linked immunosorbent assay, including high sensitivity, real-time monitoring, and no requirement for labeling.

Kinetic data from optical biosensors are generally obtained with the concentration of the ligate in excess over the immobilized ligand and thus effectively constant throughout the experiment. Under these pseudo-first-order reaction conditions the entire binding data should be described by the integrated form of the rate equation (Eq. [3]).

$$R_t = (R_{\text{eq}} - R_0)[1 - \exp(-k_{\text{on}}t)] + R_0 \quad [3]$$

In this equation,  $R_0$  is the initial instrument response,  $R_t$  is the response at time  $t$ ,  $R_{\text{eq}}$  is the maximal response, and  $k_{\text{on}}$  is the pseudo-first-order rate constant. It has been noted, however, that data are often

<sup>1</sup> To whom correspondence should be addressed.

ill-described by Eq. [2] and are better fitted by the addition of a second exponential term (3–6) (Eq. [4]). This effect is particularly pronounced at higher ligate concentrations.

$$R_t = A[1 - \exp(-k_{on(1)}t)] + B[1 - \exp(-k_{on(2)}t)] + R_0. \quad [4]$$

In Eq. [4] the instrument response,  $R_t$ , varies with two apparent association rate constants ( $k_{on(1)}$  and  $k_{on(2)}$ ); the magnitudes of the two phases are  $A$  and  $B$ , respectively, such that  $R_{eq} = R_0 + A + B$ . The faster rate ( $k_{on(1)}$ ) is found to correspond most closely to the rate constant for the interaction in solution (4, 5, 7). The slower process has been suggested to arise from steric hindrance (4, 7, 8) or diffusion limitations (9–11), but is generally accepted to be a property of the biosensor method and so provides little or no information on the intrinsic bimolecular interaction. It is important to note that Eq. [4] is an empirical solution to the analysis of biosensor data and that there is (as yet) no firm theoretical basis to justify the use of a second association rate constant.

To analyze such data, we and others (6, 10, 12, 13) have described the use of nonlinear regression to equations such as Eq. [4], in order to extract the required rate constants. In this paper we adopt an alternative approach using linear regression to analyze just the initial portion of the binding curve. We show how this analysis can be used to determine the association rate constant, and demonstrate the application of this to the interaction between the proteinase inhibitor chymotrypsin inhibitor 2 (CI-2)<sup>2</sup> and immobilized chymotrypsin. This analysis procedure is more simple than fitting the full association profile, requires less data collection time, and makes fewer assumptions about the functional form of the association profile.

## MATERIALS AND METHODS

### Materials

All chemicals used were of analytical reagent grade. Phosphate-buffered saline (PBS) tablets and  $\alpha$ -chymotrypsin were obtained from Sigma Chemical Co. (Poole, UK). Surfact-Amps 20 was purchased from Pierce & Warriner (Chester, UK). Recombinant CI-2 was prepared as described by Jandu *et al.* (14). An amine coupling kit [containing 1-ethyl-3-(3-dimethylaminopropyl) carbodiimide (EDC), *N*-hydroxysuccinimide (NHS), and 1 M ethanalamine, pH 8.5] and IAsys carboxymethyl dextran (CMD) cuvettes were from Affinity Sensors (Bar Hill, Cambridge, UK). PBS/T buffer was

prepared by the addition of 0.05% (v/v) Surfact Amps 20 to PBS buffer, pH 7.4.

### Operation of the Optical Biosensor System

The optical evanescent biosensor IAsys (Affinity Sensors) was used for the investigation into the initial rate analysis. The IAsys instrument utilizes a cuvette system in which a Peltier unit maintains a constant temperature and a stirrer ensures that mass transport effects are minimized. The principles of this biosensor are described elsewhere (15, 16). Essentially the binding of one biomolecule in solution to another attached to a carboxymethyl dextran matrix, itself linked to the sensor surface, causes a change in refractive index and/or thickness. This change is detected by the biosensor provided it occurs within the evanescent field (which extends a few hundred nanometers from the sensor surface).

### Chymotrypsin Immobilization to the CMD Matrix

Chymotrypsin was coupled using carbodiimide chemistry in which the carboxyl groups on the dextran are activated with an EDC/NHS solution for 8 min in preparation for reaction with lysine residues on chymotrypsin. The EDC/NHS solution was then replaced with PBS/T for 5 min to establish a preimmobilization baseline response on the biosensor. Immobilization was initiated by the addition of 50  $\mu\text{g/ml}$  of chymotrypsin in 10 mM acetate buffer, pH 6.0, to the cuvette and allowing the interaction to proceed for 10 min. This pH was found to give the maximal electrostatic concentration into the negatively charged dextran matrix for chymotrypsin (data not shown). After immobilization, the chymotrypsin solution was replaced by an ethanolamine wash for 2 min to quench residual NHS esters. The cuvette was finally washed with PBS/T to establish a postimmobilization response level. The amount of ligand immobilized can be calculated using the difference in the pre- and postimmobilization responses by the relationship that 1 ng protein  $\text{mm}^{-2}$  gives a response of 163 arc s on the IAsys instrument (1).

### Determination of the Capacity of Immobilized Chymotrypsin

To determine the capacity of the immobilized chymotrypsin for CI-2, a saturating concentration (6.7  $\mu\text{M}$ ) of CI-2 was allowed to bind for 10 min to obtain a saturating equilibrium response. This was achieved by adding 20  $\mu\text{l}$  of 67  $\mu\text{M}$  CI-2 to 180  $\mu\text{l}$  of PBS/T in the cuvette. After the incubation time had elapsed, the CI-2 solution in the cuvette was replaced with PBS/T and the dissociation followed for 5 min. The immobilized chymotrypsin was regenerated using 2 mM HCl for 2 min. Four washes of 200  $\mu\text{l}$  PBS/T were then performed fol-

<sup>2</sup> Abbreviations used: CI-2, chymotrypsin inhibitor 2; PBS, phosphate-buffered saline; EDC, 1-ethyl-3-(3-dimethylaminopropyl) carbodiimide; NHS, *N*-hydroxysuccinimide; CMD, carboxymethyl dextran.

lowed by a final wash with 180  $\mu\text{l}$  of PBS/T in preparation for the next CI-2 solution.

### *Binding of CI-2 to Immobilized Chymotrypsin to Determine the Association Rate Constant by Initial Rate Analysis*

A range of CI-2 concentrations from 1 to 200 nM were allowed to bind for 1 min to the immobilized chymotrypsin and then regenerated using 2 mM HCl for 2 min. Four washes of 200  $\mu\text{l}$  PBS/T were then performed followed by a 5-min reequilibration in 180  $\mu\text{l}$  PBS/T and this cycle was repeated for the remainder of the CI-2 concentrations. For example, the data for 5 nM binding were achieved by the addition of 20  $\mu\text{l}$  of 50 nM CI-2 to the cuvette containing 180  $\mu\text{l}$  of PBS/T.

### *Initial Rate Analysis for the Binding of CI-2 to Immobilized Chymotrypsin*

Linear regression analysis was performed on the initial linear portion of the interaction data and used to determine the association rate constant as outlined in the following theoretical considerations section.

## THEORETICAL CONSIDERATIONS FOR INITIAL RATE ANALYSIS

The derivation of the integrated rate equation for use with IAsys and other optical biosensors has been described (4) and is shown in Eq. [5].

$$R_t = \frac{R_{\max}[L]}{K_D + [L]} (1 - \exp(-k_{\text{ass}}[L] + k_{\text{diss}})t). \quad [5]$$

Here  $R_{\max}$  is the maximum capacity of the immobilized ligand and  $[L]$  is ligate concentration. The term  $R_{\max}[L]/K_D + [L]$  is equivalent to the term  $(R_{\text{eq}} - R_0)$  in Eq. [3]. Differentiating Eq. [5] with respect to time gives

$$\begin{aligned} \frac{dR}{dt} &= \frac{R_{\max}[L]}{K_D + [L]} (k_{\text{ass}}[L] + k_{\text{diss}}) \\ &\times \exp((-k_{\text{ass}}[L] + k_{\text{diss}})t). \end{aligned} \quad [6]$$

At time  $t = 0$  and by application of Eq. [2], Eq. [6] simplifies to

$$\frac{dR}{dt} = \frac{R_{\max}[L]}{K_D + [L]} (k_{\text{ass}}[L] + k_{\text{diss}}) = R_{\max}[L]k_{\text{ass}}. \quad [7]$$

Thus, a plot of initial rate against ligate concentration results in a straight line whose slope is equal to  $R_{\max} \cdot k_{\text{ass}}$  and has an intercept of 0.

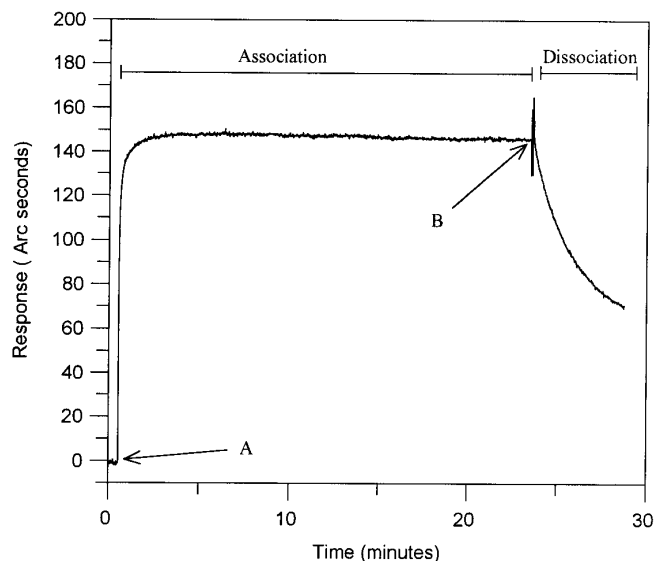


**FIG. 1.** A plot generated by the biosensor in “real time” showing the saturation of the immobilized chymotrypsin by CI-2 binding as a plateau value on the association region. Dissociation is also shown as a drop in response when the ligate solution is replaced with buffer. The addition of CI-2 is indicated by A and the buffer replacement by B.

## RESULTS

Successful application of Eq. [7] requires knowledge of the maximal binding capacity. The capacity of immobilized chymotrypsin for CI-2 was determined from the equilibrium response obtained under saturating conditions of CI-2. Figure 1 shows the interaction profile obtained at a saturating concentration of 6.7  $\mu\text{M}$  CI-2. Saturation of the vacant chymotrypsin sites is shown by the plateau at 140 arc s. Figure 1 also shows the dissociation of bound CI-2 from chymotrypsin as a decrease in response when the CI-2 solution is replaced with PBS/T buffer. This dissociation can be used to determine the dissociation rate constant ( $k_{\text{diss}}$ ) if required (6, 13). While this is not needed for the association rate constant determination, it does allow the equilibrium dissociation constant,  $K_D$ , to be calculated from Eq. [2].

The initial binding data used to calculate the association rate constant are shown in Fig. 2. For clarity, this plot just shows the first 20 s of the binding profile; at the lower ligate concentrations, the initial slope was calculated using up to 1 min of response data in order to provide greater precision. It can be seen that at high CI-2 concentration the data are linear over a shorter time period than at lower ligate concentrations. This increased curvature of the data at these higher concentrations therefore reduces the number of data points that can be used for linear regression.

To judge the accuracy of using linear regression to find the initial slope, and to determine the data range

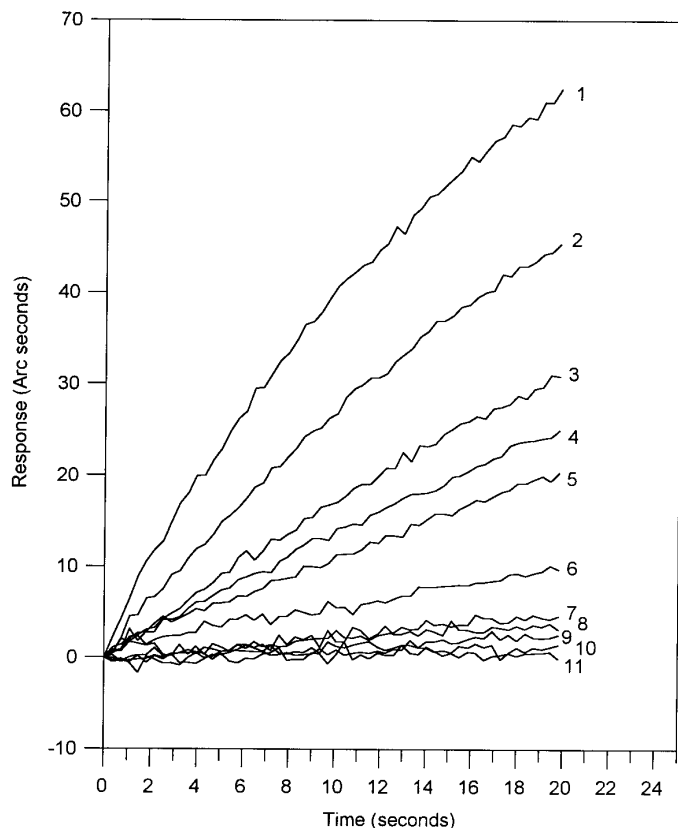


**FIG. 2.** Overlay of the initial portion of association data for CI-2 binding to immobilized chymotrypsin at a range of concentrations: 1, 200 nM; 2, 150 nM; 3, 100 nM; 4, 75 nM; 5, 50 nM; 6, 25 nM; 7, 10 nM; 8, 7.5 nM; 9, 5 nM; 10, 2.5 nM; 11, 1 nM.

that should be used for such analyses, we modeled the binding event using a first-order association curve (Eq. [3]) that had equally spaced time data. A theoretical data set was calculated where the initial rate was defined to be 1.0, and linear regression analysis was performed using various portions of the data that corresponded to increasing percentages of the maximal binding response. A plot of the slope from linear regression versus the data up to a set percentage of the  $R_{\max}$  value is shown in Fig. 3. This figure reveals that the initial rate analysis always underestimates the true initial slope. The value obtained is 90% accurate providing <19% of the maximal response is taken and 95% accurate if <10% of the maximal response is used. The maximal response at high concentrations is known from saturation experiments (Fig. 1), and so the data range used for the linear regression analysis should correspond to no more than 10–19% of this in order to obtain 95–90% accuracy.

The initial rate was determined at a variety of CI-2 concentrations ensuring that the data were analyzed over the linear portion of the binding profiles. A plot of the initial rate against ligate concentration produces a

straight line through the origin as shown in Fig. 4. The slope of this line is equal to  $R_{\max} \cdot k_{\text{ass}}$  (Eq. [7]) and gave a value of  $1.84 \pm 0.03 \times 10^7 \text{ arc s s}^{-1} \text{ M}^{-1}$ . Using the  $R_{\max}$  value determined from Fig. 1, the association rate constant for the immobilized chymotrypsin/CI-2 interaction can be calculated to be  $1.1 \pm 0.02 \times 10^5 \text{ M}^{-1} \text{ s}^{-1}$  under these experimental conditions. The dissociation rate constant was derived by application of Eq. [8] to the dissociation data in Fig. 1.

$$R_t = (R_0 - R_\infty)[\exp(-k_{\text{diss}}t)] + R_\infty. \quad [8]$$

In this equation  $R_0$  is the initial response,  $R_\infty$  the final response, and  $k_{\text{diss}}$  the dissociation rate constant. The dissociation rate constant from Fig. 1 was found to be  $7.5 \pm 0.2 \times 10^{-3} \text{ s}^{-1}$ , making the calculated  $K_D$  value equal to  $68 \pm 3 \text{ nM}$ .

## DISCUSSION

To our knowledge, linear regression analysis of the initial binding rate has not previously been used to determine the association rate constant for the interaction of biomolecules using an optical biosensor. Initial rate analysis has, however, been used for concentration analysis. Holwill *et al.* (17) have used initial rate analysis to determine the concentration of active D1.3 Fv in broth and buffer. Linear regression has also been used

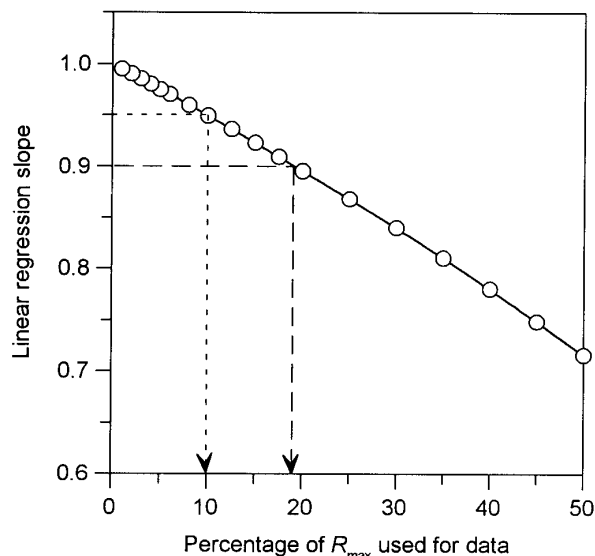


**FIG. 3.** Analysis of the effect of taking varying amounts of data describing a first-order process and fitting the initial data by linear regression. Simulated data that had a theoretical initial rate of 1.0 were generated at equal time intervals. Groups of data that started at zero time and corresponded to varying percentages of the maximal response were taken, and the slopes of these data were calculated. The figure illustrates the fractions of the total response that correspond to 90 and 95% of the theoretical value.

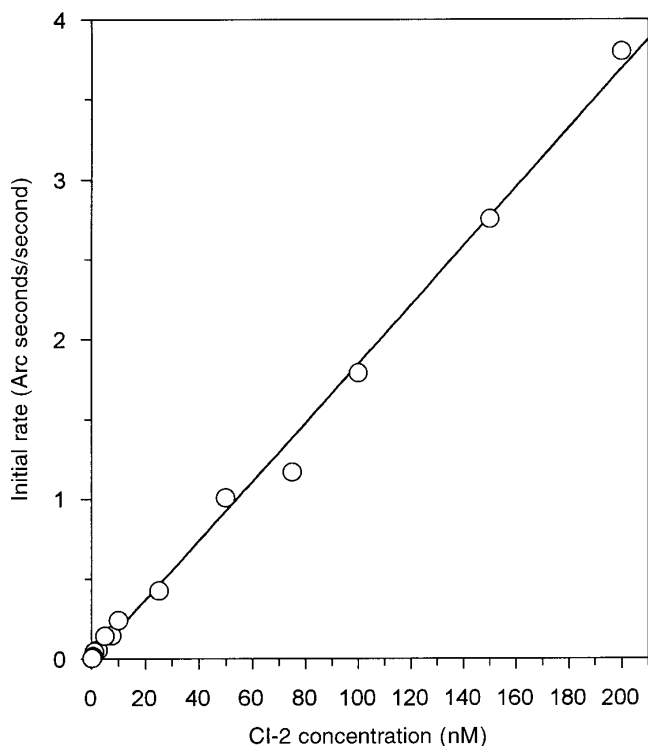


**FIG. 4.** Plot of initial binding rate of CI-2 against CI-2 concentration. The association rate constant can be calculated from the slope as in Eq. [7].

to determine the active concentration of antibodies in buffer provided that mass transport limiting conditions prevail, i.e., under high ligand immobilization levels (18). The mass transport limitation ensures that the rate is only dependent upon the antibody concentration and not the affinity of the interaction.

Data from the biosensor were linear over the initial binding profile and were found to be proportional to the concentration of CI-2 used, as expected by the derivation of Eq. [7]. This proportionality allowed a plot of initial rate against CI-2 concentration to be constructed and its slope determined. From analysis of these data it was possible to derive an association constant which was found to be comparable to that obtained from analysis of the complete binding curve at a similar immobilization level (7).

It has been well documented that data from optical biosensors often do not follow the expected Langmuir kinetics. Instead, a second exponential term in the integrated rate equation is required to accurately describe the binding data, which involves a second slower binding phase as described by Eq. [4] (3–6). However, this equation does not have a strict theoretical basis, and so it is possible to question the significance of the parameter values derived from such analyses. Various suggestions have been made to explain why biosensor

data, under certain circumstances (typically at higher ligate concentrations), display seemingly multiphase association kinetics (3–6). We have described how one contributory factor is steric crowding, where initial binding causes physical occlusion of some binding sites within the crowded surface matrix (4). Binding to the less accessible sites then either requires dissociation of already-bound material followed by rearrangement and rebinding and/or is slower due to restricted access to these sites (a diffusion limitation). Collection of just the initial portion of the association profile allows the situation to be analyzed before steric crowding occurs. It is therefore possible that such analyses offer advantages over fitting the entire association profile under circumstances where these data deviate from a simple exponential relationship (Eq. [3]).

The analysis of just the initial binding events simplifies matters by recording data only during the more rapid early binding phase. A further advantage is that the kinetics of the reaction can be determined faster than from exponential curve fitting of the entire binding profile as less data points are needed. The requirement to determine  $R_{\max}$  accurately by saturation of the immobilized ligand may be considered a disadvantage, but only if insufficient ligate is available to ensure saturation over a reasonable time period.

Initial rate analysis as described above does not directly provide a value for the dissociation rate constant. However, the dissociation rate constant can easily be measured directly in the same experiment as that required for  $R_{\max}$  determination (Fig. 1) and in combination with the derived association constant allows full characterization of the binding interaction.

One further advantage of using initial rate measurements occurs when the affinity of the interaction is high. To ensure a complete description of the kinetic parameters of the interaction, ligate concentrations below the  $K_D$  value may be required. In these circumstances, binding may result in significant depletion of ligate, which would result in second-order kinetics and severely complicate the analysis. Initial rate analysis intrinsically involves binding of only a small fraction of the ligate and so always follows pseudo-first-order kinetic equations.

The use of initial rate analysis of the initial binding data generated from optical biosensors allows the rapid determination of the association rate constant. In addition, this analysis eliminates interpretational complications arising from nonideal behavior often observed for the binding of moderate to high ligate concentrations for longer interaction times. The saturation of the immobilized ligand to obtain  $R_{\max}$  also allows the dissociation rate constant to be determined under conditions where rebinding of the dissociated ligate is minimized. The overall dissociation equilibrium constant  $K_D$  can thus be determined rapidly.

## REFERENCES

1. Yeung, D., Gill, A., Maule, C. H., and Davies, R. J. (1995) *Trends Anal. Chem.* **14**(2), 49–56.
2. Malmborg, A. C., Michaëlsson, A., Ohlin, B., Jansson, B., and Borrebaeck, CAK. (1992) *Scand. J. Immunol.* **35**, 643–650.
3. George, A. J. T., French, R. R., and Glennie, M. J. (1995) *J. Immunol. Methods.* **XX**, 51–63.
4. Edwards, P. R., Gill, A., Pollard-Knight, D. V., Hoare, M., Buckle, P. E., Lowe, P. A., and Leatherbarrow, R. J. (1995) *Anal. Biochem.* **231**, 210–217.
5. Corr, M., Slanetz, A. E., Boyd, L. F., Jelonek, M. T., Khilko, S., Al-Ramadi, B. K., Kim, Y. S., Maher, S. E., Bothwell, A. L. M., and Marguiles, D. H. (1994), *Science* **265**, 946–949.
6. O'Shannessy, D. J., Brigham-Burke, M., Soneson, K. K., Hensley, P., and Books, I. (1994) *Anal. Biochem.* **212**, 457–468.
7. Edwards, P. R., Lowe, P. A., and Leatherbarrow, R. J. (1997) *Mol. Recog.*, in press.
8. Karlsson, R., Roos, H., Fägerstam, L., and Persson, B. (1994) *Methods.* **6**(2), 99–120.
9. Schuck, P. (1996) *Biophys. J.* **70**, 1230–1249.
10. Glasser, R. W. (1993) *Anal. Biochem.* **213**, 152–161.
11. Felder, S., Zhou, M., Hu, P., Urena, J., Ullrich, A., Chaudhuri, M., White, M., Shoelson, S. E., and Schlessinger, J. (1993) *Mol. Cell. Biol.* **13**, 1449–1455.
12. Calakos, N., Bennett, M. K., Peterson, K. E., and Scheller, R. H. (1994) *Science* **263**, 1146–1149.
13. Karlsson, R. (1994) *Anal. Biochem.* **221**, 142–151.
14. Jandu, S. K., Ray, S., Brooks, L., and Leatherbarrow, R. J. (1990) *Biochemistry* **29**, 6264–6269.
15. Cush, R., Cronin, J. M., Stewart, W. J., Maule, C. H., Molloy, J., and Goddard, N. J. (1993) *Biosens. Bioelectron.* **8**, 347–353.
16. Buckle, P. E., Davies, R. J., Kinning, T., Yeung, D., Edwards, P. R., Pollard-Knight, D., and Lowe, C. R. (1993) *Biosens. Bioelectron.* **8**, 355–363.
17. Holwill, I., Gill, A., Harrison, J., Hoare, M., and Lowe, P. A. (1996) *Process Control Qual.* **209**, (in press).
18. Karlsson, R., Fägerstam, L., Nilshans, H., and Persson, B. (1993) *J. Immunol. Methods* **166**, 75–84.